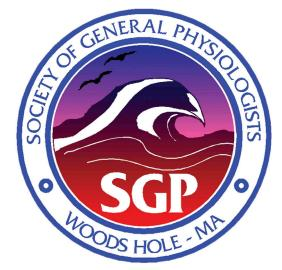
ABSTRACTS OF PAPERS AT THE SIXTY-NINTH
ANNUAL MEETING OF THE SOCIETY
OF GENERAL PHYSIOLOGISTS

Macromolecular Local Signaling Complexes

Marine Biological Laboratory

Woods Hole, Massachusetts 16–20 September 2015



Organized by

HENRY COLECRAFT, ANDREW MARKS, and STEVEN MARX

1. A New Role for Na_V1.5: Preserving Intercellular Adhesion Strength. E. AGULLO-PASCUAL,¹ T. ARCOS,¹ X. LIN,¹ L. BU,¹ L. BIN,¹ M. ZHANG,¹ M. CERRONE,¹ S. FOWLER,¹ B. MURRAY,² A.S. TE RIELE,² C.A. JAMES,² C. TICHNELL,² H. CALKINS,² E. ROTHENBERG,¹ D.P. JUDGE,² and M. DELMAR,¹ New York University School of Medicine, New York, NY 10016; ²Johns Hopkins University School of Medicine, Baltimore, MD

The intercalated disc (ID), the region at the cell ends connecting two adjacent myocytes, allows mechanical and electrical coupling between cells. Other molecules essential for normal cardiac electrophysiology, including voltage-gated sodium channels (VGSCs), also localize at the ID. Different studies suggest extensive cross-talk and functional interdependence between the complexes. Here, we test the hypothesis that VGSCs are important to maintain cell–cell adhesion.

HEK293 cells were stably transfected to express $Na_V1.5$ (VGSC α subunit). Intercellular adhesion was tested by dispase assay. Cell monolayers were detached from plates with dispase and subjected to mechanical stress, and the number of fragments was counted. Cells expressing $Na_V1.5$ were more resistant to mechanical stress compared with control $(2.5 \pm 0.5 \text{ fragments}, n = 20 \text{ vs. } 25.3 \pm 3.6 \text{ fragments}, n = 16, \text{ respectively}). <math>Na_V1.5$ -expressing cells knocked down for the desmosomal protein plakophilin-2 (PKP2) were used as positive control and also showed weak intercellular adhesion $(12.8 \pm 2.3 \text{ fragments}, n = 20)$. Similar experiments performed on HL-1 cells knocked down for Nav1.5 or PKP2 showed similar results: 1.0 ± 0.0 , 39.8 ± 1.8 , and $51.8 \pm 6.3 \text{ fragments}$ in control, Nav1.5, and PKP2, respectively.

To complement these observations, we performed three-dimensional super-resolution fluorescence microscopy (3D-SRFM) in human induced pluripotent stem cell–derived cardiac myocytes (hIPSC-CM) from an arrhythmogenic cardiomyopathy patient carrying a mutation in SCN5A (gene coding for Na_V1.5). 3D-SRFM images (20-nm resolution in XY; 40 nm in Z) showed reduced number of Na_V1.5 clusters within 500 nm of N-cadherin plaques: 4,719 (n=20 images) and 1,746 clusters (n=21) in control and patient, respectively. Importantly, the number of N-cadherin clusters also decreased: 26,793 versus 13,983 in control and patient, respectively (P < 0.0001). Cluster sizes were not different between groups.

We show reduced intercellular adhesion strength associated with loss of Nav1.5, and a structural dependence of N-Cadherin on the integrity of Nav1.5. We propose that VGSCs are not only important for cardiac electrophysiology but also to support intercellular adhesion strength.

2. Biochemical Analysis of the Regulation of Kv7 Channels by PIP_2 and Calmodulin. CRYSTAL R. ARCHER, BENJAMIN T. ENSLOW, PAMELA A. REED,

and MARK S. SHAPIRO, UT Health Science Center San Antonio, STRF, San Antonio, TX 78229

Kv7 (M-type, KCNQ) K+ channels are expressed throughout the brain and play dominant roles in control of neuronal excitability because of their threshold of activation at subthreshold potentials. M-channels have been identified as therapeutic targets to reduce neuronal excitability in certain brain disorders, such as epilepsy and chronic pain. We seek to elucidate the molecular mechanisms of Kv7 channel regulation by second messengers used in their regulation by $G_{\alpha/11}$ -coupled receptors, and the structural determinants of the channels that are involved. Activation of Gq/11-mediated signals results in the hydrolysis of the membrane-bound lipid, phosphatidylinositol 4,5-bisphosphate (PIP₂), and an increase in Ca²⁺-bound calmodulin (Ca²⁺/CaM) that is associated with M-current suppression and enhanced neuronal excitability. The structure of Kv7 channels consists of a six transmembrane-spanning region with an extended cytoplasmic carboxy terminus containing a proximal "regulatory domain" with two alpha helices and two regions enriched in basic amino acids that are thought to be the principal sites of PIP₂- and CaM-mediated binding. Recently, we examined the affinity of PIP₉ to this regulatory domain spanning from the S6-TMD to the end of the B-helix domain (KCNQ-RD). By monitoring the shift in intrinsic protein fluorescence, we observed a change in the conformation of KCNQ-RD by the presence of the water-soluble analog, diC8-PIP₂. Fluorescence polarization assays showed a reduction of anisotropy of a fluorescently labeled PIP₂ analog with increasing KCNQ-RD titrations. These results support that PIP₉ directly binds the KCNQ-RD. Using other biochemical methods, we are also showing PIP₂ interacting with a complex of KCNQ-RD in complex with CaM. Because CaM also binds in this region, we hypothesize that the interactions of CaM and PIP₉ with Kv7 channels are allosterically or sterically coupled, such that the binding of one molecule affects the affinity of binding of the other, or affects the efficacy of its action in modulating channel gating.

3. Detecting the Stoichiometry of Macromolecular Complexes in Live Cells Using Fluorescence Resonance Energy Transfer. MANU BEN-JOHNY, DANIEL N. YUE, and DAVID T. YUE, Calcium Signals Lab, Johns Hopkins University, Baltimore, MD 21218

The stoichiometry of molecular interactions represents a fundamental parameter for understanding cellular signaling events. Although conceptually simple, experimentally deducing this key metric in the context of live cells can be a daunting challenge for macromolecular complexes. For example, the ubiquitous Ca²⁺sensing molecule calmodulin (CaM) is known to serve as a crucial regulator of voltage-gated Ca²⁺ channels. However, the number of CaM molecules that interact

with the channel has long remained controversial. Functional studies have argued that a single CaM is sufficient for channel regulation, whereas structural and biochemical studies have argued that multiple Ca²⁺/ CaM molecules can interact with the channel. To address this conundrum, we devised a novel strategy using fluorescence resonance energy transfer (FRET), a phenomenon whereby a donor fluorescent molecule nonradiatively transfers energy to a nearby acceptor molecule. Typically, FRET efficiency between fluorophore-tagged molecules could be measured from either acceptorcentric (Three-Cube) or donor-centric (E-FRET) perspectives. Here, we exploit a fundamental asymmetry between these metrics to estimate the stoichiometry of binding: If a binding interaction is multimeric, then the ratio of maximal FRET efficiencies, as measured by Three-Cube and E-FRET methods, will equal the ratio of donors to acceptors present in the complex. This theoretical principle is validated using concatemers of CFP and YFP molecules and by analyzing CaM interaction with multiple segments of the neck region of unconventional myosin V. Finally, the application of this methodology to the voltage-gated Ca²⁺ channel complex reveals a 1:1 stoichiometry of CaM interaction under Ca²⁺-free conditions. However, upon the addition of Ca²⁺, a second CaM molecule may be recruited to the channel complex. This Ca²⁺-dependent switch in the stoichiometry of CaM interaction may represent a novel mode of channel signaling and information transfer. Overall, this assay adds to a burgeoning toolkit to pursue quantitative biochemistry of signaling complexes in live cells.

4. Novel Intact Ex Vivo Preparation of Pressurized Intracerebral Arterioles and Capillaries Reveals Conducted Upstream Vasodilation and Endothelium-dependent Vasodilation Amplification by Inward Rectifier Potassium Channels. FABRICE DABERTRAND, JOSEPH E. BRAYDEN, and MARK T. NELSON, Pharmacology, University of Vermont College of Medicine, Burlington, VT 05405

In brain parenchymal arterioles (PAs), endothelial-dependent vasodilators act in part by stimulating intermediate (IK) and small conductance (SK) Ca²+-sensitive K+ channels. We hypothesized that the ensuing membrane hyperpolarization, and possibly accumulation of perivascular K+, activates endothelial cell (EC) and smooth muscle (SM) $K_{\rm ir}$ channels. We found that the $K_{\rm ir}$ channel blocker Ba^{2+} (30 μM) attenuated vasodilation in response to IK/SK channel activation by the synthetic agonist NS309.

We further explored this macromolecular signaling complex in a novel intact ex vivo preparation made by pressurizing a PA with a capillary ramification left intact and sealed by compressing its extremity with a glass micropipette. We then compared the vascular reactivity in PA and capillary plus PA (CaPA) preparations. Bath elevation of extracellular $[K^+]_e$ concentration from 3 to 10 mM, known to activate strong inward rectifier K^+ (K_{ir}) channels, caused almost a maximal dilation of arterioles in PA and CaPA preparations. Similarly, 1 μM NS309, strongly, rapidly, and reversibly dilated PA, with and without capillaries, suggesting that PA endothelial function is intact.

We then investigated the possibility of retrograde signaling from capillaries to upstream arterioles by local application of vasoactive substances. Pressure ejection of NS309 onto capillaries had no effect on PA. However, the application of 10 mM [K+]e to the capillaries led to a rapid dilatory response (lag time of <2 s) in the upstream PA (53.4 \pm 5.6%), which was abolished by Ba²+. 1 μ M prostaglandin E2 also induced upstream, Ba²+sensitive arteriolar dilation (38.6 \pm 7.3%; lag time of >8 s), which was reduced by specific genetic deletion of K_{ir} in the myocytes. These data support the concept that capillary K_{ir} channels act as K^+ sensors to initiate retrograde electrical signals, and that smooth muscle K_{ir} channels amplify endothelial IK/SK channels to dilate upstream arterioles.

Supported by National Institutes of Health (grants R01HL121706, PO1HL-095488, and R37-DK-053832), Totman Medical Research Trust, Fondation Leducq, and the United Leukodystrophy Foundation.

5. A Nonlinear Dependence for Arrhythmogenesis on Gene Expression in Timothy Syndrome. IVY E. DICK, ROSY JOSHI-MUKHERJEE, WANJUN YANG, and DAVID T. YUE, Department of Biomedical Engineering and Department of Neuroscience, Johns Hopkins University, Baltimore, MD 21205

Timothy syndrome (TS) is a multisystem disorder, featuring neurological impairment, autism, and cardiac action-potential prolongation with life-threatening arrhythmias. The underlying basis is a single-point mutation in Ca_V1.2 channels, either G406R or G402S. These mutations occur in either exon 8 or exon 8A, such that the expression pattern of these mutually exclusive exons significantly contributes to the overall severity of the disease in patients. Further, opposing shifts in channel activation of the two mutations results in contrasting regulatory defects, such that G402S channels suffer primarily from a lack of Ca²⁺ driving CDI, whereas G406R channels exhibit an increased channel open probability even in the Ca²⁺-inactivated state. To explore the implications of this mechanistic dichotomy, we used an established action potential model that revealed a nonlinear dependence of the action potential duration on the fraction of TS channels expressed. To explore this experimentally at the cell-network level, we variably expressed TS channels in cultured adult guinea pig ventricular myocytes. Indeed, conservative expression of TS channels yielded graded action-potential prolongation, but a small further increase led to significant arrhythmia. Such nonlinear dependence on channel expression imparts an important principle for therapeutics: a small shift in the compliment of mutant versus wild-type channels may impart a significant clinical improvement. A possible therapeutic strategy would therefore use methods to alter the splice expression pattern of the mutually exclusive exons 8/8A. In all, we have demonstrated the power of in-depth biophysical analysis to inform on therapeutic strategy.

6. Role of Mitochondrial Reactive Oxygen Species in Age-dependent Loss of *C. Elegans* Muscle Function. FRANCES M. FORRESTER, ¹ ALISA UMANSKAYA, ¹ WENJUN XIE, ¹ STEVEN REIKEN, ¹ ALAIN LACAMPAGNE, ^{1,2} and ANDREW R. MARKS, ¹ ¹Department of Physiology and Cellular Biophysics, Columbia University, New York, NY 10032; ²Institut National de la Santé et de la Recherche Médicale (INSERM U1046)/Université, Montpellier I, Montpellier, France

The ryanodine receptor (RyR) is a conserved, calcium release channel located in the endo/sarcoplasmic reticulum (ER/SR). RyR1 is the predominant isoform in skeletal muscle and a crucial mediator of excitationcontraction coupling. It comprises a macromolecular complex that includes the channel-stabilizing protein calstabin1. Posttranslational modification of RyR1 results in calstabin1 depletion and intracellular calcium leak. In aged skeletal muscle, this leak is hypothesized to reduce the membrane potential of nearby mitochondria, which subsequently overproduce reactive oxygen species (ROS) and further oxidize RyR1, exacerbating calcium leak/muscle dysfunction. The nematode Caenorhabditis elegans is a well-established model with a short lifespan, ideal for aging studies; however, the underlying physiology of muscle dysfunction in C. elegans aging and the role of ROS are unknown. Therefore, we have characterized the role of mitochondrial ROS in age-dependent decline of C. elegans muscle function by examining the oxidation state of its RyR homologue, UNC-68, in two mitochondrial mutant strains (clk-1 and mev-1). Both strains contain electron transport chain mutations; however, *clk-1* is long-lived whereas *mev-1* is short-lived. Our data demonstrate that UNC-68 is a macromolecular complex highly homologous to RyR1; in WT aged worms, UNC-68 is oxidized and FKB-2 (calstabin1) is depleted from the channel. Additionally, FKB-2 depletion reduces peak calcium before and after caffeineinduced UNC-68 activation. Thus, we hypothesize that mev-1 mutations increase mitochondrial ROS and muscle dysfunction via oxidized leaky UNC-68 and depletion of FKB-2 earlier in life, whereas clk-1 mutations do not. Biochemical analysis reveals that although young mev-1 mutants had oxidized UNC-68 depleted of FKB-2, clk-1 UNC-68 oxidation was absent until old age. Further

studies include ROS measurements via mitochondrial-targeted, redox-sensitive GFP and locomotion assays. Our goal is to demonstrate intracellular calcium leak's importance in muscle pathophysiology and establish *C. elegans* as a tractable model of calcium signaling mechanisms therein.

7. Evolution of Excitation–Contraction Coupling in Teleost Fish: Evidence for Divergence of Fast and Slow Twitch Modes. JENS FRANCK, SARA GOOD, TIM PELLISIER, and SERGEY YEGOROV, Department of Biology, University of Winnipeg, Winnipeg, MB, Canada R3B 2E9

Excitation-contraction (EC) coupling describes the relationship between the depolarization of the muscle membrane and the subsequent contraction of the muscle cell. In skeletal muscle cells, the depolarization of the muscle membrane triggers a conformational change in the L-type calcium channel (Ca_V1.1). In skeletal muscle, the Ca_V1.1 directly interacts and mechanically gates the intracellular ryanodine receptor (RyR) channel to release calcium from the intracellular stores of the sarcoplasmic reticulum, a mechanism termed "depolarization-induced calcium release" (DICR). In contrast, the L-type channel in cardiac muscle (Ca_V1.2) opens in response to the depolarization signal, and the extracellular calcium subsequently acts as a ligand to gate open the intracellular RyR channels, a mechanism termed "calcium-induced calcium release" (CICR). The DICR mode of calcium release is believed to be a vertebrate innovation. We previously described fiber type-specific expression of RyR1 paralogs in slow twitch (ryr1a) and fast twitch (ryr1b) muscle fibers in fish (Franck et al. 1998. Amer. J. Physiol. 275:C401-C415; Darbandi and Franck. 2009. Comp. Biochem. Physiol. B. 154:443-448). More recently, it has been reported that the alpha_{1S} subunits (α_{1S}) of the multimeric Ca_V1.1 channel are also duplicated and expressed discretely in the slow twitch $(\alpha_{1S}$ -a) and fast twitch $(\alpha_{1S}$ -b) muscles of zebrafish (Schredelseker et al. 2010. Proc. Natl. Acad. Sci. USA. 107:5658–5663). The II–III loop of the α_{1s} subunit and the divergent region 1 (DR1) of RyR1 have been implicated as the domains responsible for the mechanical coupling process. Using selection analyses, we show that amino acids within the α_{1S} II-III loop and RyR1 DR1 regions are under positive selection. Additionally, the nodes leading to the fast twitch-specific genes (ryr1b and α_{1S} -b) show a greater extent of positive selection than the nodes leading to the slow twitch-specific genes (ryr1a and α_{1s} -a). Multiple sequence alignments reveal evidence for the fixation of functionally divergent amino acids in the RyR1 DR1 and α₁₈ II-III loop domains. We discuss the implications of these results and the potential for the coevolution of the functional domains responsible for the DICR mode of EC coupling in teleost fish.

8. Histone-induced Endothelial Calcium Signals: A Novel Mechanism for Detection of Tissue Injury. KALEV FREEMAN, DANIEL M. COLLIER, ADRIAN SACKHEIM, NURIA VILLALBA, ADRIAN D. BONEV, and MARK T. NELSON, *University of Vermont, Burlington, VT 05405*

Histones are released by cellular injury (e.g., trauma, infection, ischemia) and from activated neutrophils, and it was recently shown that exposure of cultured endothelial cells to histones causes Ca²⁺ overload and cell death. The effects of histones on intact vessels have not been studied, and specific ion channels involved in histone-induced Ca2+ overload are unknown. We studied spatial and temporal characteristics of endothelial Ca2+ signals after exposure of mesenteric microvessels to purified histones (Roche). Using transgenic mice with endothelial cell-specific Ca²⁺ biosensor (GCaMP5) expression, we performed spinning-disc confocal imaging of Ca2+ signals of intact endothelium under physiological conditions. Concentrations of histone equivalent to those in severe trauma patients (>20 µg/mL) rapidly caused endothelial Ca2+ overload and cell death. Surprisingly, even at histone levels equivalent to those in healthy adults (1 µg/mL), exposure induced local Ca²⁺ events, contained within endothelial microdomains. At higher concentrations (10 µg/mL), histones triggered larger, longer duration Ca2+ waves that propagate between endothelial cells. These Ca²⁺ signals appear to involve different ion channels. Both signals were unaffected by cyclopiazonic acid (CPA), arguing against IP₃ receptor-mediated Ca²⁺ events. Treatment with the transient receptor potential cation V4 channel (TRPV4) antagonist (GSK219) suppressed localized Ca²⁺ events induced by 1 μg/mL histones. In contrast, propagating Ca²⁺ events at higher histone concentrations were unaffected by GSK219 but completely eliminated by removal of extracellular Ca²⁺. In summary, histones are robust activators of endothelial Ca²⁺ signals through both TRPV4-dependent and TRPV4-independent pathways. This suggests a novel mechanism of immuno-vascular coupling, in which histones, released by injured cells and activated neutrophils, could activate TRVP4 channels to modulate blood flow into areas of injury or inflammation. Higher levels of circulating histones in severe trauma or sepsis may explain endothelial barrier breakdown, disseminated intravascular coagulation, multi-organ failure, and circulatory collapse, and could provide a therapeutic target.

Sponsored by National Institutes of Health and Totman Trust.

9. Isoproterenol Promotes Rapid Ryanodine Receptor Movement to BIN1 Organized Dyads. YING FU,¹ SEIJI SHAW,¹ ROBERT NAAMI,¹ CARESSE VUONG,¹ and TINGTING HONG,^{1,2} ¹ Cedars-Sinai Heart Institute and ²Department of Medicine, Cedars-Sinai Medical Center, Los Angeles, CA 90048

Introduction

In mammalian ventricular cardiomyocytes, excitation-contraction coupling relies on calcium-induced calcium release (CICR) at dyads, which consist of ryanodine receptors (RyRs) at sarcoplasmic reticulum apposing Cav1.2 channels at t-tubules. Sympathetic tone regulates myocardial CICR through β-adrenergic receptor (β-AR) signaling-mediated phosphorylation of dyadic proteins. Phosphorylated RyRs (P-RyRs) have increased calcium sensitivity and open probability (Marx et al. 2000. *Cell.* 101:365–376), improving CICR gain at a cost of receptor instability. Given that BIN1 organizes t-tubule microfolds (Hong et al. 2014. *Nat. Med.* 20:624–532) and traffics Cav1.2 channels (Hong et al. 2010. *PLoS. Biol.* 8:e1000312), we asked if RyR organization can be dependent on BIN1 microdomains.

Objective

We determined whether β -AR-stimulated P-RyR localization and function can be regulated by BIN1 microdomains.

Methods and Results

Using spinning-disc confocal and super-resolution direct stochastic optical reconstruction microscopy (dSTORM) imaging, we identified that BIN1 microdomains are enriched with both P-RyR and Cav1.2. P-RyR coimmunoprecipitates with cardiac t-tubule BIN1+13+17, particularly after acute β-AR activation (1 µmol/L isoproterenol for 5 min). In addition to phosphorylating RyRs, isoproterenol also redistributes BIN1 to t-tubules, which recruits P-RyRs, thereby improving CICR gain and calcium transients. In cardiac-specific heterozygous Bin1-deleted myocytes, isoproterenol phosphorylates RyRs but fails to concentrate BIN1 to t-tubules, impairing P-RyR recruitment into dyads. The resultant outside accumulation of uncoupled P-RyRs increases the incidence of spontaneous calcium release.

Conclusions

Upon β -AR activation, reorganization of BIN1 microdomains recruits P-RyR into dyads, increasing CICR gain while preserving electrical stability. When BIN1 is reduced as in acquired heart failure, impaired BIN1 microdomain formation results in accumulation of uncoupled leaky P-RyRs.

10. Contractile Pericytes Determine the Direction of Blood Flow at Capillary Bifurcations. ALBERT L. GONZALES,¹ THOMAS A. LONGDEN,¹ BO SHUI,² MICHAEL I. KOTLIKOFF,² and MARK T. NELSON,¹ ¹Department of Pharmacology, University of Vermont, Burlington, VT 05404; ²Department of Biomedical Sciences, College of Veterinary Medicine, Cornell University, Ithaca, NY 14853

Pericytes, as part of the neurovascular unit, contribute to functional hyperemia, the process whereby metabolically active neurons stimulate an increase in local capillary blood flow necessary to maintain the momentto-moment delivery of nutrients and removal of waste. Similar to vascular smooth muscle cells, pericytes can express the contractile machinery capable of generating focal constrictions within the capillary bed. The goal of the current study was to identify the ion channels involved in contraction and to elucidate the functional role of pericytes in regulating capillary blood flow. We tested the hypothesis that pericytes localized at capillary junctions are capable of controlling the direction of flow in the capillary bed. Using immunohistochemistry, we observed that only a subpopulation of pericytes localized to first- and second-order branches of capillaries proximal to feeding arterioles express contractile elements, such as α-actin, Ca_v1.2, and TRPM4, and only these cells contracted to the thromboxane A2 analog, U46619. Notably, contractile junctional pericytes exhibited asymmetric coverage and constriction at capillary bifurcations. Using a novel transgenic mouse expressing a genetically encoded Ca²⁺ biosensor in contractile pericytes (acta2-GCaMP5-mCherry), we observed that local Ca2+ dynamics were also asymmetric in junctional pericytes. In addition, we pharmacologically isolated IP₃R- and Cav1.2-mediated Ca²⁺ events, but did not observe Ca²⁺ released from ryanodine receptors in junctional pericytes. Using in vivo multiphoton microscopy, we observed asymmetrical movement of red blood cells at bifurcations and U46619-induced pericyte contraction decreased and symmetrized junctional blood flow, suggesting that pericytes play a role in controlling the directional flow of blood within the capillary bed.

Supported by Totman Medical Research Trust, Fondation Leducq, American Heart Association (14POST20480144), and National Institutes of Health (grants T32HL-007594, P01HL-095488, R37DK-053832, R01HL-121706, and R24HL-120847).

11. Effectors of the PLC-based Light-signaling Pathway across Distantly Related Microvillar Photoreceptors. KEVIN GONZÁLEZ,^{1,3} CAMILO GALINDO,¹ ENRICO NASI,^{2,4} and MARÍA DEL PILAR GOMEZ,^{1,3} ¹Departamento de Biología, ²Instituto de Genética, and ³Centro Internacional de Fisica Bogotá, Universidad Nacional de Colombia, Bogotá, D.C., Colombia; ⁴Marine Biological Laboratory, Woods Hole, MA 02543

"R-opsins" comprise a large group of light-sensing molecules found in visual receptors of arthropods and mollusks, and in circadian receptors of vertebrates. They signal via a G_q , which is coupled to the phosphoinositide cascade; however, downstream effector mechanisms remain controversial, and conflicting physiological evidence has been obtained in different species. *Drosophila melanogaster* is the only organism in which

the molecular underpinnings of this light-transduction pathway have been studied systematically. To assess the generality of the proposed scheme, a broader phylogenetic coverage would be desirable, encompassing widely divergent species. We focused on the microvillar photoreceptors from the retina of a mollusk (Pecten irradians) and the neural tube of a primitive chordate (Branchiostoma floridae). A homology-based bioinformatics search was carried out on the transcriptome of Pecten retina and the genome of Branchiostoma, targeting the light-regulated enzyme and putative light-activated ion channels. PCR amplifications and RACE extensions using Pecten retina cDNA yielded two PLC-β isoforms; one of them, related to Drosophila norpA, was localized in the microvillar photoreceptors by in situ hybridization and immunofluorescence. A different PLC-B ortholog was identified in amphioxus neural tube. A TRPC was found in Pecten but failed to localize to the retina layer comprised of microvillar photoreceptors. Of several TRP orthologs cloned from Branchiostoma neural tube cDNA, two express in photosensitive neurons, although nonexclusively: a TRPC and a TRPA (a subclass that includes some cationic channels gated by calcium). The latter result dovetails with recent evidence that the photo-conductance of Branchiostoma microvillar photoreceptors is activated by the Ca increase resulting from light-induced release from internal stores. Collectively, the observations strengthen the notion that the molecular machinery for phototransduction across microvillar photoreceptors of phylogenetically disparate species follows a common blueprint.

Supported by Colciencias Contract 0813 to Centro Internacional de Fisica.

12. Regulation of Endothelial TRPV4 Channel Activity in the Cerebral Circulation. OSAMA F. HARRAZ,¹ THOMAS A. LONGDEN,¹ ADRIAN D. BONEV,¹ SWAPNIL K. SONKUSARE,¹ KALEV FREEMAN,^{1,2} and MARK T. NELSON,^{1,3} ¹Department of Pharmacology and ²Department of Surgery, College of Medicine, University of Vermont, Burlington, VT 05405; ³Institute of Cardiovascular Sciences, University of Manchester, Manchester, UK

The transient receptor potential vanilloid 4 (TRPV4) channel in the mesenteric endothelium plays a pivotal role in mediating Ca²⁺ entry leading to membrane hyperpolarization. We previously showed that pial arterial endothelial cells (pECs) in the cerebral circulation express functional TRPV4 channels, which are less sensitive to the TRPV4 agonist GSK1016790A (GSK101) when compared to their peripheral counterparts. This suggests that TRPV4 channels are differentially regulated, depending on the vascular bed and/or cellular environment. Here, we used patch-clamp electrophysiology and ECs freshly isolated from cerebral pial arteries and capillaries (cECs) to explore possible mechanisms underlying disparate functional regulation of TRPV4

channels. Perforated patch-clamp electrophysiology indicated differential responsiveness to GSK101 between pECs and peripheral ECs, whereas conventional wholecell recordings in pECs revealed a TRPV4 current that was comparable to that in peripheral ECs. Inclusion of ATP in the pipette solution rendered pECs less sensitive to GSK101, suggesting a role for protein kinase inhibitory regulation of TRPV4. Consistent with this hypothesis, suppression of protein kinase G (PKG) using KT5823 or Rp-8-Br-cGMP enhanced GSK101 responsiveness in pECs in the perforated configuration. Similarly, cEC TRPV4 channels were sensitive to GSK101 in the whole-cell but not the perforated configuration. This sensitivity in the whole-cell configuration was prevented when cECs were dialyzed with ATP, in line with findings in pECs. In conclusion, TRPV4 channels are differentially regulated in the cerebral circulation because of, at least in part, a modulatory role of protein kinase G. This suppressive role of PKG signaling may represent a mechanism underlying the tighter control over TRPV4 channel activity, which has broad implications for TRPV4 channel control of diverse cell types beyond endothelial cells.

Supported by Totman Medical Research Trust, Fondation Leducq, and National Institutes of Health (grants R01 HL121706, PO1 HL-095488, and R37-DK-053832).

13. Saturated Fat Causes Cardiac Mitochondrial Dysfunction and Abnormal Calcium Homeostasis by Activating PKC and NOX2. LEROY C. JOSEPH, EMANUELE BARCA, PRAKASH SUBRAMANYAM, MICHAEL KOMROWSKI, HENRY M. COLECRAFT, MICHIO HIRANO, and JOHN P. MORROW, Division of Cardiology, Columbia University Medical Center, New York, NY 10032

Introduction

Saturated fat increases the risk of cardiovascular disease and sudden cardiac death. The mechanisms involved are unclear. We hypothesized that saturated fat could induce mitochondrial dysfunction and abnormal calcium homeostasis in cardiomyocytes.

Methods

Isolated ventricular myocytes from adult mice were exposed to the saturated fat palmitate or the monounsaturated fat oleate (as a control) to determine the effects on reactive oxygen species (ROS), mitochondrial function, and sarcoplasmic reticulum calcium release (sparks).

Results

Palmitate activates PKC in cardiomyocytes; oleate does not. Total cellular ROS and mitochondrial ROS are increased by palmitate. Inhibitors of PKC or NAPDH oxidase 2 (NOX2) prevent the increase in ROS. Palmitate

also depolarizes the mitochondrial inner membrane and decreases mitochondrial oxygen consumption. Mitochondrial dysfunction is prevented by inhibition of PKC or NOX2. Palmitate-induced NOX2 activation causes mitochondrial calcium overload in intact cardiomyocytes by increasing sparks.

Conclusion

In cardiomyocytes, saturated fat induces mitochondrial ROS. Mitochondrial ROS is amplified by NOX2 via PKC activation, resulting in greater mitochondrial ROS generation and mitochondrial dysfunction. Activation of NOX2 causes abnormal sarcoplasmic reticulum calcium leak. NOX2 inhibition could be a promising therapy for heart disease caused by diabetes or obesity.

14. High Saturated Fat Diet Increases Ventricular Ectopy by Activating NADPH Oxidase 2. LEROY C. JOSEPH, PRAKASH SUBRAMANYAM, HENRY M. COLECRAFT, and JOHN P. MORROW, *Division of Cardiology, Columbia University Medical Center, New York, NY 10032*

Introduction

Dietary saturated fat is associated with an increased risk of arrhythmia and sudden cardiac death. We investigated if a high fat diet is sufficient to cause heart rhythm abnormalities before the onset of obesity, and the molecular mechanisms involved.

Methods

Isolated ventricular myocytes from wild-type or NAPDH oxidase 2 (NOX2) KO mice were exposed to the saturated fat palmitate or oleate (the major component of olive oil) to determine the effects on reactive oxygen species (ROS). We recorded heart rhythm in wild-type mice before and after a high fat diet (60% fat) composed either of saturated fat (palm oil) or monounsaturated fat (olive oil).

Results

Palmitate increases ROS in wild-type ventricular cardiomyocytes, which is inhibited by the NOX2 inhibitor apocynin or a specific peptide inhibitor. Cardiomyocytes with genetic ablation of NOX2 do not have palmitate-induced ROS. After baseline heart rhythm recordings on regular chow, mice were fed a high fat diet for 4 weeks. Neither diet resulted in significant weight gain. On the saturated fat diet, mice had a significant increase in ventricular ectopy in the form of premature ventricular complexes (PVCs) and a significant increase in QT interval. The olive oil diet did not cause an increase in ventricular ectopy or QT interval. Cardiac lysates from mice on high saturated fat diet show increased NOX2 activity. Apocynin, an inhibitor of NOX2, prevents PVCs and LQT caused by a high saturated fat diet.

Conclusion

Saturated fat causes oxidative stress in cardiomyocytes. A high saturated fat diet is sufficient to cause electrophysiologic abnormalities in vivo, by activating NOX2.

15. Polycystin 2, and the Effects on Cardiac Calcium–Contraction Coupling with Aging. IVANA Y. KUO,¹ ANDREA T. KWACZALA,² LILY NGUYEN,¹ STUART G. CAMPBELL,² and BARBARA E. EHRLICH,¹ Department of Pharmacology and ²Department of Biomedical Engineering, Yale University, New Haven, CT 06520

Cardiac dysfunction is the main cause of mortality in the commonly occurring genetic disorder autosomal dominant polycystic kidney disease (ADPKD). However, how the mutations in the polycystins predispose ADPKD patients to cardiac disorders before development of renal dysfunction is unknown. We investigate the effect of decreased polycystin 2 (PC2) levels, a calcium channel that interacts with the ryanodine receptor, on myocardial function. We hypothesize that heterozygous PC2 mice (Pkd2+/-) undergo cardiac remodeling stemming from changes in calcium handling that progress with aging. In 5-month-old mice, Pkd2+/- cardiomyocytes have altered calcium handling, independent of desensitized calcium-contraction coupling. Paradoxically, in Pkd2+/- mice, PKA phosphorylation of phospholamban was decreased, whereas PKA phosphorylation of troponin I was increased, explaining the decoupling between calcium signaling and contractility. In silico modeling supported this relationship. Echocardiography measurements showed that Pkd2+/- mice have increased left ventricular ejection fraction after stimulation with isoproterenol (ISO), a β-adrenergic receptor (βAR) agonist. Importantly, the Pkd2+/- mice were normotensive and had no evidence of renal cysts. The hypersensitivity to ISO was even more pronounced in 9-month-old Pkd2+/- mice, corresponding with a shift to the β AR-2 pathway. Intriguingly, the older Pkd2+/mice also displayed features of dilated cardiomyopathy (DCM) and decreased baseline cardiac function. The DCM features are consistent with what is observed in a subset of human ADPKD patients without renal dysfunction. In conclusion, our results show that decreased PC2 levels alter the sensitivity of the calciumcontractility apparatus. Moreover, there is increased sensitivity to the β-adrenergic receptor signaling pathway and evidence of DCM in aged Pkd2+/- mice. We propose that PC2 levels in the heart directly contribute to cardiac remodeling in ADPKD patients in the absence of renal dysfunction.

16. Acute Lithium Administration Enhances Gq/PLC-mediated Signaling. MARIA PAULA LANDINEZ,^{1,2} SARA DURAN,^{1,2} TOMAS OSORNO,^{1,2} MARÍA DEL PILAR GOMEZ,^{3,4} and ENRICO NASI,^{2,4} ¹Departamento de Biología, ²Centro Internacional de Fisica, and ³Instituto

de Genética, Universidad Nacional de Colombia, Bogotá, D.C., Colombia; ⁴Marine Biological Laboratory, Woods Hole, MA 02543

Although lithium has long been one of the most widely used pharmacological agents in psychiatry, its mechanisms of action at the cellular and molecular level remain poorly understood. One of the putative targets of Li+ is G protein-mediated signaling, and in particular the phosphoinositide pathway. Evidence has been garnered previously on Li⁺ effects both on inositol lipid metabolism and on Ca mobilization after metabotropic-receptor activation in cell populations; however, information on physiological effects at the single-cell level is lacking. In primary photosensitive neurons of an early chordate, which have been documented to respond via the activation of a Gq/PLC pathway, we uncovered a robust enhancement of the receptor current after acute Li+ administration at high doses. To extend the generality of such an observation to mammalian cells and to Li+ concentrations that approach levels of therapeutic interest, we then focused on HEK293 cells in culture, which had been reported to express M1AchR metabotropic receptors. First, Western blot and immunofluorescence assays were used to corroborate the expression of key signaling elements of the PLC pathway in HEK293, such as G_q and PLC- β 1. To ascertain the presence of a G protein-coupled ionic conductance, we used whole-cell patch-clamp recording, and observed inward membrane currents triggered by dialysis of GTP-γ-S. Stimulation of endogenous muscarinic receptors with carbachol evoked a similar inward current and a dose-dependent mobilization of Ca, as determined with fluorescent indicators; this was caused by release from internal stores and proved susceptible to the PLC antagonist U73122. Li⁺ exposure reproducibly potentiated the Ca response in a concentration-dependent manner, extending to the low millimolar range, i.e., close to its therapeutic doses. These observations document an up-regulation of Gq/PLC/IP3-mediated signaling by acute exposure to lithium, manifesting itself in defined physiological responses monitored in individual cells.

Supported by DIB-Universidad Nacional de Colombia, Hermes No. 28407.

17. Nanoscale Visualization of Functional Adhesion/ Excitability Nodes at the Intercalated Disc. ALEJANDRA LEO-MACIAS, ESPERANZA AGULLO-PASCUAL, JOSE L. SANCHEZ-ALONSO, SARAH KEEGAN, XIANMING LIN, FENG-XIA LIANG, YURI E. KORCHEV, JULIA GORELIK, DAVID FENYO, ELI ROTHENBERG, and MARIO DELMAR, The Leon H. Charney Division of Cardiology, Center for Health Informatics and Bioinformatics, and Department of Biochemistry and Molecular Pharmacology, New York University School of Medicine, New York, NY 10016; Department of Cardiac Medicine, Imperial Centre for Translational and Experimental Medicine, National Heart and Lung Institute, and ⁵Division of Medicine, Imperial College, Hammersmith Campus, London, United Kingdom

Intercellular adhesion and electrical excitability are considered separate cellular properties, achieved by independent macromolecular complexes. Studies of myelinated fibers, however, have shown that proteins responsible for electrical conduction (i.e., voltage-gated sodium channels [VGSCs]) aggregate with cell adhesion molecules at discrete subcellular locations, such as the nodes of Ranvier. Demonstration of a similar macromolecular organization in cardiac muscle is missing. Here, we show that anatomical adhesion/excitability nodes are present at the site of contact between cardiac myocytes (the intercalated disc [ID]). We used a combination of nanoscale imaging techniques including single-molecule localization microscopy (SMLM), electron microscopy (EM), and "angle view" scanning patch clamp, together with mathematical simulations to reveal the existence of distinct ID hubs populated by clusters of both the adhesion molecule N-cadherin and the cardiac sodium channel Na_V1.5. Our results demonstrate that N-cadherin acts as an attractor for Na_v1.5, that the Na_V1.5 molecules in these clusters are major contributors to the cardiac sodium current (I_{Na}), and that clustering facilitates the regulation of Na_V1.5 by its molecular partners. We speculate that adhesion/excitability nodes are key sites for cross talk of the contractile and electrical molecular apparatus. These nodes may represent the structural substrate underlying cases of cardiomyopathies in patients with mutations in molecules of the VGSC complex.

A. Leo-Macias and E. Agullo-Pascual contributed equally to this work.

18. Potassium Sensing by Capillary K_{IR} Channels Regulates Cerebral Blood Flow. THOMAS A. LONGDEN,¹ FABRICE DABERTRAND,¹ ALBERT L. GONZALES,¹ MASAYO KOIDE,¹ and MARK T. NELSON,^{1,2} ¹Department of Pharmacology, College of Medicine, University of Vermont, Burlington, VT 05405; ²Institute of Cardiovascular Sciences, University of Manchester, Manchester, UK

Brain parenchymal arterioles (PAs) feed a vast capillary network, with capillary endothelial cell (cEC) density matching that of neurons in cortical structures (García-Amado and Prensa. 2012. *PLoS ONE.* 7:e38692). This angioarchitecture suggests that capillary ECs play an essential role in the signaling mechanisms coupling neuronal activity to increases in local cerebral blood flow. We therefore tested the hypothesis that the capillary network can detect neuronal activity—through activation of strong inward rectifier K⁺ (K_{IR}2) channels by external K⁺—which then initiates communication to upstream PAs to cause dilation and an increase in blood flow to the capillary bed. To investigate this, ion channel

currents were measured in freshly isolated brain cECs using the patch-clamp technique, and capillary hemodynamics were observed in vivo.

cECs possessed K_{IR} currents sensitive to 100 μ M Ba²⁺, which were not present in EC $K_{IR}2.1$ knockout mice. In contrast to ECs from arteries, small- and intermediate-conductance Ca^{2+} -activated K^+ channels were absent from cECs. $K_{IR}2$ channels are activated by external K^+ and membrane hyperpolarization and, therefore, are ideally suited to sense changes in external K^+ and translate this into a regenerative hyperpolarization, which could induce vasodilation of upstream PAs. Consistent with this hypothesis, pressure ejection of 10 mM K^+ onto capillaries in vivo evoked hyperemia within seconds, which was sensitive to $100~\mu$ M Ba²⁺, and was not present in EC $K_{IR}2.1^{-/-}$ mice.

Our findings indicate that brain capillaries constitute an active sensory web, converting changes in external K⁺ into rapid "inside-out" signaling to regulate blood flow into the brain. In the context of these results, brain capillaries can be viewed as a series of electrical wires that facilitate the long-distance communication of neuronal activity to the surface vasculature.

Supported by American Heart Association (14POST20480144), Totman Medical Research Trust, Fondation Leducq, and National Institutes of Health (grants R01 HL121706, PO1 HL-095488, and R37-DK-053832).

19. CaMK2G, an Intellectual Disability Candidate Gene, Is Critical for Spatial Learning and Activity-dependent BDNF Synthesis in the Hippocampus. HUAN MA, SANDRINE SANCHEZ, ILONA KATS, BENJAMIN SUUTARI, and RICHARD W. TSIEN, NYU Neuroscience Institute, NYU Langone Medical Center, New York, NY 10016

Intellectual disability (ID) is a disorder characterized by significant limitations in both intellectual function and adaptive behavior. We have identified γ CaMKII, encoded by an ID candidate gene CaMK2G, as a Ca²⁺/ CaM shuttle protein that supports membrane signaling to nuclear CREB and gene expression. Various players in this pathway (Ca_V1 channels, γCaMKII, βCaMKII, calcineurin, and CaMKIV) are encoded by genes implicated in neuropsychiatric disorders that often coexist with ID, including autism spectrum disorder and major depression disorder. To ask whether there is a link between this pathway and ID as well as other neuronal disorders, we probed yCaMKII-mediated excitationtranscription (E-T) coupling and its consequences in mice lacking γCaMKII. The anxiety level of γCaMKII^{-/-} mice was normal in open field or elevated zero maze tests. However, γCaMKII^{-/-} mice showed repetitive and depression-like behavior in the marble bury and forced swim test. Because the intellectual functioning in people with ID is often limited, we examine the learning ability of γCaMKII^{-/-} mice using a Morris water maze

(MWM). Strikingly, γCaMKII^{-/-} mice showed impaired ability to find a hidden platform, as well as an inability to recall that location after platform removal. To validate this further, we tested mice in a radial arm maze, which invokes different motivations and motor systems. Consistent with our findings in MWM, γ CaMKII^{-/-} mice also showed significantly impaired reference memory in a radial arm maze. Because CREB-dependent gene expression is critical for neuronal plasticity, we asked whether this process is impaired in $\gamma \text{CaMKII}^{-/-}$ mice. Indeed, BDNF, a CREB-targeted gene, increased more than twofold in the hippocampus with MWM training, which was prominently absent in γCaMKII^{-/-} mice. Importantly, the inhibition of BDNF expression was not caused by impairment of the MAPK pathway, suggesting a specific and critical role of yCaMKII-mediated E-T coupling in spatial learning.

20. Determinants on Neuronal Voltage-gated Calcium Channel (Ca,2.2) Responsible for Functional Interaction with Auxiliary $\alpha_2\delta$ -1 Subunit. SIHUI MA¹ and HENRY M COLECRAFT, 1.2 ¹Department of Pharmacology and Molecular Signaling and ²Department of Physiology and Cellular Biophysics, Columbia University, New York, NY 10032

Auxiliary α₉δ-1 subunit of the voltage-gated calcium (Ca_V) channel plays an important role in Ca_V channel regulation and is implicated in a variety of cardiovascular and neurological diseases. However, how $\alpha_0\delta$ -1 binds to and regulates Ca_V channels and the precise mechanisms by which $\alpha_2\delta$ -1 dysfunction causes diseases are unclear. Here, we investigated the determinants on neuronal Ca_V2.2 (α_{1B}) channels responsible for functional interaction with α₉δ-1 subunit in HEK293 cells and scrutinized the mechanisms underlying $\alpha_0\delta$ -1 regulation of Ca_v2.2. Whole-cell electrophysiology experiments showed that $\alpha_2\delta$ -1 caused a dramatic four- to fivefold increase in Ca_V2.2 whole-cell current amplitude compared with channels reconstituted with $\alpha_{1B} + \beta_{2a}$ alone in HEK293 cells. Using a quantum dot-labeling technique, we demonstrated that this increase in current was wholly accounted for by an increase in channel surface expression. Optical pulse-chase experiments showed that $\alpha_2\delta$ -1 increased α_{1B} surface density solely through reducing the α_{1B} rate of endocytosis, and had no significant impact on its rate of forward trafficking. To map the determinants on α_{1B} that are critical for $\alpha_2\delta$ -1 functional interaction, we inserted a small epitope tag into a number of judiciously selected extracellular regions of the α_{1B} subunit. By assessing the accessibility of the inserted tags to quantum dot and by determining whether or not they disrupted $\alpha_9\delta$ -1 modulation of whole-cell currents, we identified that an intact S5-S6 loop of α_{1B} domain III was important for $\alpha_9\delta$ -1 regulation. Alanine-scanning mutagenesis on this loop revealed discrete residues necessary for $\alpha_9\delta$ -1 functional interaction. Collectively, our study provides novel insights into mechanisms underlying $\alpha_2\delta$ -1 regulation of Ca_V channels and offers a new target site on Ca_V2.2 for development of future therapeutics in treating $\alpha_2\delta$ -1–associated diseases.

21. cAMP Microcompartments in *Drosophila melanogaster* Motor Neurons. ISABELLA MAIELLARO,¹ MARTIN J. LOHSE,¹ ROBERT J. KITTEL,² and DAVIDE CALEBIRO,¹ Institute of Pharmacology and Toxicology, Rudolf Virchow Center, and ²Department of Neurophysiology, Institute of Physiology, University of Würzburg, Germany

Cyclic AMP (cAMP) plays a major role in synaptic plasticity in vertebrate and invertebrate neuronal systems. Although cAMP signaling has been shown to be compartmentalized, the existence and properties of cAMP microdomains in neurons are highly debated. The role of this study was to investigate the spatiotemporal dynamics of cAMP signaling at the Drosophila melanogaster neuromuscular junction, where octopamine binding to its receptors has been shown to cause cAMPdependent synaptic plasticity. For this purpose, we generated a transgenic *Drosophila* expressing the cAMP sensor Epac1-camps in motor neuron. This allowed us to directly follow the octopamine-induced cAMP signals in real time by fluorescence resonance energy transfer (FRET) in different compartments of the motor neuron (i.e., cell body, axon, boutons). We found that octopamine induces a steep cAMP gradient from the synaptic bouton (high cAMP) to the cell body (low cAMP), which was caused by higher PDE activity in the cell body. High octopamine concentrations evoked a response also in the soma. Notably, these signals were independent and isolated from each other. Moreover, the application of octopamine by iontophoresis to single synaptic boutons induced bouton-confined cAMP signals. These data reveal that a motor neuron can possess multiple and largely independent cAMP-signaling compartments, and provide a new basis to explain how cAMP could control neurotransmission at a level of a single synapse.

22. K_{ATP} Channel Is Activated by Insulin through PI3K in CA3 Rat Hippocampal Neurons. SERGIO MÁRQUEZ-GAMIÑO,¹ KARLA S. VERA-DELGADO,² ARMANDO OBREGÓN-HERRERA,³ CIPRIANA CAUDILLO-CISNEROS,¹ and CARLOS G. ONETTI,⁴¹Departamento de Ciencias Aplicadas al Trabajo, ²Departamento de Enfermería y Obstetricia, Sede Guanajuato, and ³Departamento de Biología, Universidad de Guanajuato, Gto., México; ⁴Centro Universitario de Investigaciones Biomédicas, Universidad de Colima, Col., México.

Insulin is involved in several functional processes at the central nervous system, including regulation of feeding behavior and energy balance, as well as synaptic plasticity. The union of insulin to its receptors (IR) causes K_{ATP} channel activation through an intracellular pathway of phosphoinositide-3-kinase (PI3K), in hypothalamic neurons. Both IR and K_{ATP} channels are expressed at hippocampus neurons. Our aim was to characterize the insulin action on the K_{ATP} channel activity and PI3K pathway participation in CA3 rat hippocampal neurons.

Experiments were carried out in pyramidal cells from slices of hippocampus from 4-weeks-old Wistar male rats. Single-channel current records using patch-clamp technique were done in CA3 neurons at room temperature (20–22°C). Open-state probability (P_O) values were calculated from 30-second current records at different membrane potentials. Pipette filling solution (mM): 140 KCl, 1 MgCl₂, and 10 HEPES, pH 7.3 with KOH. Hippocampus slice perfusion solution (mM): 130 NaCl, 3 KCl, 1 CaCl₂, 1 MgCl₂, and 10 HEPES pH 7.4 with NaOH; p-glucose was added to this solution at 30 mM. Inside-out patch pipette internal solution (mM): 140 KCl, 1 MgCl₂, 2 EGTA, and 10 HEPES, pH 7.2 with KOH.

Single-channel currents were abolished by adding 100 μM glibenclamide, in inside-out configuration, and channel activity was recovered after washout. Insulin, at 60 and 120 nM, increased K_{ATP} channel open-state probability. In the presence of insulin and D-glucose, 200 μM tolbutamide inactivated K_{ATP} channels. Adding 10 μM of the PI3K inhibitor LY294002, in the presence of 120 nM insulin, reduced P_O of K_{ATP} channels.

In the pyramidal cells of the CA3 region of the hippocampus, insulin activates K_{ATP} channels in the presence of 30 mM glucose, an action mediated by PI3K. This result allows us to propose a mechanism in which insulin and glucose are involved in the regulation of K_{ATP} channel excitability in the rat hippocampus neurons.

Supported by CONACyT CB-2006/56541. Correspondence to Sergio Márquez-Gamiño: smgamino@fisica.ugto.mx

23. Characterization of the Cardiac Phenotype of Malignant Hyperthermia-associated Mutation of RyR1. JIN O-UCHI,¹ JYOTSNA MISHRA,¹ BONG SOOK JHUN,¹ STEPHEN HURST,¹ DEMING FU,¹ LUDOVIC GOMEZ,¹,² and SHEY-SHING SHEU,¹ ¹ Center for Translational Medicine, Thomas Jefferson University, Philadelphia, PA 19107; ²INSERM UMR-1060, Laboratoire CarMeN, Université Lyon 1, Faculté de Médecine Rockefeller et Charles Merieux Lyon-Sud, Lyon F-6900, France

Mutations of the type 1 isoform of the ryanodine receptor (RyR1) form "leaky" channels (high susceptibility to activation) and frequently exhibit inherited skeletal muscle (SM) disorders including malignant hyperthermia (MH) and central core disease (CCD). In addition to SM phenotypes, arrhythmias and sudden cardiac death (SCD) in MH/CCD patients are frequently

observed with anesthesia, and in the conscious condition (e.g., during exercise), without an increase in the body temperature and in the absence of hyperkalemia. These reports indicate that SCD frequently observed in patients carrying mutations with leaky RyR1 channels cannot be solely explained as a secondary effect of their SM dysfunction. However, the molecular mechanism underlying cardiac phenotypes in MH/CCD is still unknown, and the risk stratification of SCD and arrhythmias in MH/CCD has not been established. We determined previously that a low level of RyR1 is expressed in the mitochondria ("mitochondrial" RyR1 [mRyR1]), but not in the sarcoplasmic reticulum (SR) in the heart, which serves as an important mitochondrial Ca2+ influx pathway in addition to the mitochondrial Ca²⁺ uniporter complex. Here we show, using knock-in mice carrying an RyR1 mutation Y522S (YS) found in a human MH family, that YS hearts possess YS-RyR1 in mitochondria (but not in SR) and exhibit disrupted mitochondrial morphology as well as compromised mitochondrial functions with a high cellular oxidative state. We also found that YS cardiomyocytes have higher basal mitochondrial Ca²⁺ concentration, depolarized mitochondrial membrane potential, and slower cytosolic Ca²⁺ clearance compared to WT. Moreover, YS heart developed multiple ventricular extrasystoles in response to β-adrenergic stimulation under ex vivo Langendorff perfusion. In conclusion, these results indicate that chronic mitochondrial Ca2+ overload via leaky mutant mRyR1 damages cardiac mitochondrial functions/structures, reduces cytosolic Ca²⁺-buffering capacity, and induces cellular oxidation, which facilitates arrhythmogenic outbursts in MH/CCD under acute catecholaminergic stress.

24. Pushing the Limits of Voltage-Clamp Fluorometry: Short-Range Distance Assignment in Proteins under Physiological Conditions. ANTONIOS PANTAZIS and RICCARDO OLCESE, Department of Anesthesiology & Perioperative Medicine, Division of Molecular Medicine, David Geffen School of Medicine, University of California, Los Angeles, Los Angeles, CA 90095

Fluorescence approaches using Förster resonance energy transfer are invaluable for measuring long intramolecular and intermolecular distances. However, there is a paucity of experimental approaches to accurately determine short (<25-Å) distances under physiologically relevant conditions. To address this shortcoming, we developed an experimental and theoretical framework to determine the distance between an introduced Cys (labeled with fluorophores of different lengths) and a Trp, which provides state-dependent, collisional quenching of the label. We combined this quantitative approach with voltage-clamp fluorometry to determine the distances between the BK channel voltage-sensor transmembrane helices in the resting and active states,

revealing the molecular transitions underlying voltage sensing in a ubiquitous regulator of cellular excitability in the membrane environment, under physiological conditions.

We resolved voltage-evoked fluorescence deflections of tetramethylrhodamine fluorophores (in order of increasing length: TMR-6'-M; TMR-5'-M; TMR-6'-C2-M, TMR-5'-C2-M, and a mixture of TMR-5/6'-C6-M isomers), labeling the extracellular positions of helices S0, S1, or S2, as they were quenched by Trp-203, at the extracellular flank of helix S4. These data ($n \ge 4$ cells per condition) were fit to distance distributions (C α -xanthene centroid) for each fluorophore, constructed using molecular dynamics simulations (MMFF94,100 ps) to account for fluorophore flexibility and map fluorescence data to protein label site/Trp quencher distances.

At rest, S0, S1, and S2 are approximately equidistant from S4: S0–S4 mean = 11.9 Å; 95% CI (10.4 Å, 12.9 Å); S1–S4 = 12.4 Å (12.3 Å, 12.5 Å); S2–S4 = 11.5 Å (8.8 Å, 12.3 Å). Upon voltage-sensor activation, S1 and S4 diverge to 18.3 Å (17.7 Å, 20.0 Å) apart, whereas the S0–S4 and S2–S4 distances exceed 24 Å. Combining this new information with our current knowledge on BK and other K^+ channels, we constructed a structural model for the BK voltage sensor in resting and active states.

This approach complements FRET-based techniques for distance measurements under physiological conditions. We are validating this approach on *Ci*-VSP, which has a known atomic structure, and synthetic polyproline peptides.

25. Ae4 (Slc4a9) Is an Electroneutral Cl⁻/Na⁺-HCO₃⁻ Exchanger. GASPAR PEÑA-MÜNZENMAYER, YASNA JARAMILLO, JAMES E. MELVIN, and MARCELO A. CATALÁN, Secretory Mechanisms and Dysfunction Section, National Institute of Dental and Craniofacial Research, National Institutes of Health, Bethesda, MD 20892

Transcellular Cl- movement across acinar cells is the rate-limiting step for salivary gland fluid secretion. Recently, we demonstrated that Ae4 (Slc4a9) anion exchangers are expressed in mouse submandibular acinar cells where they contribute to Cl--dependent fluid secretion. Ae4 null mice show reduced HCO₃⁻-dependent Cl⁻ uptake, in keeping with Cl⁻/HCO₃⁻ exchanger activity. However, the functional properties and subcellular localization of Ae4 in different tissues remain controversial. It has been proposed that Ae4 mediates Cl⁻/HCO₃⁻ exchange or Na⁺-HCO₃⁻ cotransport. We studied the biophysical proprieties of Ae4 to better understand how it promotes saliva secretion. CHO cells transiently transfected with mouse Ae4 cDNA and native submandibular acinar cells were loaded with BCECF, SBFI, or SPQ to monitor intracellular pH, Na+, and Cl⁻ changes, respectively. Intracellular alkalinization (HCO₃⁻ uptake) and Cl⁻ exit were observed in cells exposed to a HCO₃⁻-containing, low Cl⁻ bath solution,

consistent with $\text{Cl}^-/\text{HCO}_3^-$ exchanger activity. $\text{Cl}^-/\text{HCO}_3^-$ exchange was absent in an extracellular Na⁺-free bath solution. Na⁺ uptake was enhanced in a low Cl^- bath solution, and its uptake was insensitive to EIPA (a Na⁺/H⁺ exchanger inhibitor). Our results show that Na⁺ and HCO_3^- are transported in the same direction, whereas Cl^- movement occurs in the opposite direction, demonstrating a $\text{Cl}^-/\text{Na}^+\text{-HCO}_3^-$ exchange mechanism and ruling out Na⁺-HCO₃⁻ cotransport. Finally, Ae4 activity was insensitive to changes in the membrane potential, suggesting that mouse Ae4 is an electroneutral $\text{Cl}^-/\text{Na}^+\text{-HCO}_3^-$ exchanger.

26. Translating Empirical Values into Reinterpretable Data: The Case of Postsynaptic Density Property Modifiers and Mechanisms of Synaptic Plasticity. PETER PENNEFATHER^{1,2} and WEST SUHANIC, ¹ IgDial Inc., Toronto; ²Leslie Dan Faculty of Pharmacy, University of Toronto, Toronto, Canada?

Biophysical simulations suggest that intrinsic variability in synaptic receptor density and distribution or presynaptic quantal size and release properties get harmonized into the appearance of a much simpler but functionally equivalent system made up of identical synapses. The influence of this intrinsic variability on synaptic plasticity modulation, making it subject to adaptive evolution, remains to be determined. New imaging methods applied at the level of individual synapses now make that question tractable. Optophysiological methods and targeted optical probes enable direct optical tracking of synaptic plasticity phenomena and associated changes in the synthesis, turnover in movements of distinct synaptic molecules at specific synapses. New microscopy methods now allow resolution of individual synapses in macroscopic structures in unprecedented detail and number using increasingly open and accessible methodologies. However, these tools generate large amounts of challenging data. This is a microcosm of larger pragmatic challenges in modern science: (a) sharing and building upon data concerning complex system dynamics; (b) using all the data to constrain abstracted representations of system dynamics; (c) replicability and openness to reinterpretation; and (d) accounting for misinterpreted or corrupted data and their impact on conclusions. We present a technical solution to that challenge. The method and system first atomize data by recording a data quanta to a dedicated digital archive. This archive will contain bytes representing a value and a recording record. The recording record is open-ended but minimally sufficient and necessary for allowing evaluation of the repeatability and integrity of the value. Therefore, each will be different from any other in terms of, for example, timing, location, perspective, etc. The associated bytes will also be unique and can be hashed to generate a digital unique identifier that also specifies data integrity. This then

facilitates pragmatic rediscovery, reconsolidation, and repurposing of data using standard indexing, search, and retrieval methods.

27. Myocardial Expression of Sap97 Is Important for Beta-adrenergic Regulation of Murine Heart Rate. B. ROSINSKI, H. MUSA, M. IBRAHIM, T. NDUKWE, G. GUERRERO-SERNA, T. HERRON, and J. ANUMONWO, Department of Internal Medicine (Cardiovascular) and Department of Molecular Integrative Physiology, University of Michigan, Ann Arbor, MI 48109

Background

Synapse-associated protein 97 (Sap97) is a membrane-associated guanylate kinase-like protein that clusters ion channels, beta-1 adrenergic receptor (β1-AR), and enzymes. In the heart, such macromolecular complexes of proteins are important for regulating electrical impulses. We have examined the role of *Sap97* deletion in beta-adrenergic regulation of the murine heart rate (HR).

Methods and Results

A murine model of cardiac-targeted Sap 97 gene deletion was generated using the Cre-Lox system. ECGs were carried out on anesthetized wild-type (WT) and Sap97 knockout (Sap97KO) under control conditions and after isoproterenol (ISO) challenge (1.5 mg/kg; SC). In WT mice, with ISO there was an increase in HR that returned to baseline with a biphasic profile; an initial rapid decline (<5 minutes) and a longer-lasting decline to baseline (\sim 20 minutes). Sap 97KO animals also showed an initial rapid decline in HR but a more prolonged decline, which remained at 25% above baseline (n = 3.3). In a different set of mice, telemetry was performed on conscious animals, which were challenged with ISO after Sap 97 ablation (n = 4). HR in the mice showed a similar biphasic response, remaining 35% above baseline after Sap97KO (P = 0.047). Atrial tissue from WT and Sap 97KO mice were examined for changes in components of β1-AR signaling, which might impact HR. In Sap97KO compared to WT, protein levels (relative to GAPDH) showed ~86% reduction in Sap97 from 0.7 ± 0.1 to 0.1 ± 0.05 (P = 0.008). In contrast, there was an \sim 57% increase in β 1-AR protein, from 0.3 ± 0.1 to 0.7 ± 0.1 (P = 0.003). However, PKA and Cav1.2 protein levels were relatively unchanged (n = 3-6).

Conclusion

Our model of targeted Sap97 ablation is important for understanding the role of Sap97 in the regulation of the cardiac impulse. Furthermore, abnormal Sap97 expression alters β 1-AR expression, which is important for autonomic regulation of HR.

28. Reduced IP₃-mediated Ca²⁺ Signaling in Syndromic and Nonsyndromic Forms of Autism Spectrum Disorders.

GALINA SCHMUNK,^{1,3} RACHEL L. NGUYEN,³ KENNY KUMAR,³ DAVE FERGUSON,^{1,3} IAN PARKER,^{1,3,4} and J. JAY GARGUS,^{1,2,3} ¹Department of Physiology and Biophysics and ²Division of Human Genetics & Genomics, Department of Pediatrics, School of Medicine, ³Center for Autism Research and Treatment, and ⁴Department of Neurobiology and Behavior, School of Biological Sciences, University of California, Irvine, Irvine, CA 92697

There are no known biomarkers or therapeutics targeted to core deficits of autism spectrum disorder (ASD) because of limited understanding of molecular causes of this common severe disability. Genetic evidence supports disrupted Ca2+ signaling, known to be ubiquitously involved in neuronal function, in ASD etiology. Using "optical patch-clamp" techniques, we had discovered kinetic alterations in Ca²⁺ channel function of inositol trisphosphate receptors (IP₃Rs) of fibroblasts derived from patients with three monogenic forms of ASD: fragile X (FXS) and tuberous sclerosis TSC1 and TSC2 syndromes. Although there was no difference in Ca²⁺ stores, unitary event amplitudes, openings, or latency to first opening elicited by photolysis of caged IP₃, all ASD model cells showed a shorter (15 vs. 32 ms) open channel time constant and a dramatic reduction in the apparent number of release sites.

A highly reproducible FLIPR assay was devised to screen for this molecular difference between the ASD models and controls using ATP activation of purinergic receptors, and here this assay was extended to fibroblasts obtained from deeply phenotyped, whole-genome sequenced subjects with "typical ASD" enrolled through our center. Fibroblasts from the majority showed the same defective Ca²⁺ signaling compared to age-, sex-, and ethnically matched controls as originally observed in the monogenic models. In view of the extreme heterogeneity of ASD, these preliminary results strongly suggest that dysregulated IP₃R signaling lies at a central node in a molecular pathway leading to core features of autism. It additionally may account for non-neuronal ASD symptoms (gastrointestinal and immunological) and potentially known environmental components, as ER serves as an environmental stress sensor. Fibroblasts, routinely acquired as clinical specimens, may thus offer a promising technique in conjunction with behavioral testing for early detection of ASD, and potentially for highthroughput screening of novel therapeutic agents.

29. Dissecting Roles of Distinct α_{1C} Intracellular Domains in Functional Targeting of $Ca_V1.2$ Channels to Dyadic Junctions in Cardiomyocytes. PRAKASH SUBRAMANYAM, DONALD D. CHANG, and HENRY M. COLECRAFT, Department of Physiology and Cellular Biophysics, Columbia University Medical Center, New York, NY 10032

Cardiac excitation–contraction (EC) coupling relies on Ca²⁺-induced Ca²⁺ release (CICR) enabled by an intimate

relationship between L-type (Ca_V1.2) channels and ryanodine receptors (RyRs) at dyadic junctions. How Ca_V1.2 channels target in proximity to RyRs at dyads is unknown, but likely involves protein interactions mediated by one or more intracellular loops of Ca_V1.2 pore-forming α_{1C} subunit. We hypothesized that overexpressing α_{1C} intracellular loops that play a critical role in Ca_V1.2/RyR functional colocalization would disrupt CICR in cardiomyocytes. We overexpressed fluorescent protein-tagged α_{1C} intracellular loops and termini (NT, I–II, II–III, III–IV, CT) in adult rat cardiomyocytes and assessed their impact on field stimulation-evoked rhod-2-reported Ca²⁺ transients and other determinants of CICR (I_{CaL} , t-tubule structure, SR Ca^{2+} content, spontaneous Ca²⁺ sparks). Overexpressed I–II and CT uniquely disrupted EC coupling as characterized by two distinct signatures: a sharp augmentation in CICR failure, and an increased propensity for arrhythmic Ca²⁺ transients. Surprisingly, both I-II and CT paradoxically induced a substantial rise in frequency of spontaneous Ca²⁺ sparks. The effects of I–II on CICR and Ca²⁺ sparks were phenocopied by overexpressing the 18-residue AID peptide responsible for high affinity auxiliary Ca_Vβ binding to α_{1C} . Overexpressing a mutated AID (YWI/AAA) that no longer binds Ca_Vβ produced normal CICR and spontaneous Ca²⁺ sparks. The effects of CT on CICR and spontaneous Ca²⁺ sparks were phenocopied by the distal CT that is unique to α_{1C} and contains binding sites for several signaling and scaffold proteins. Collectively, the results shed new light on molecular determinants important for Ca_V1.2 functional targeting in cardiomyocytes, and suggest a new unconventional role for functionally intact dyads as being necessary to quell spontaneous openings of RyRs.

30. Dual Ionic and Conformational Ca_V1.2 Dynamics Trigger CaMKII-mediated CREB Signaling. MICHAEL R. TADROSS, ^{1,3} BOXING LI, ² and RICHARD W. TSIEN, ^{1,2} ¹Department of Molecular and Cellular Physiology, Beckman Center, Stanford University School of Medicine, Stanford, CA 94305; ²Department of Neuroscience and Physiology, NYU Neuroscience Institute, New York, NY 10016; ³Janelia Research Campus, Howard Hughes Medical Institute, Ashburn, VA 20147

The physical logic by which molecules operate defines their computational role. Voltage-gated $Ca_V1.2$ channels are critical mediators of transcription-dependent neural plasticity, yet establishing whether they signal via Ca^{2+} influx, voltage-dependent conformational changes (V ΔC), or a more discriminating combination of the two has been equivocal. Here, we fused $Ca_V1.2$ to a ligand-gated Ca^{2+} -permeable channel, enabling independent control of nanodomain Ca^{2+} and $V\Delta C$ signals. This revealed an unexpected dual requirement: Ca^{2+} must first mobilize actin-bound CaMKII, freeing it for subsequent $V\Delta C$ -mediated accumulation—neither signal in isolation

suffices to activate CREB, a nuclear protein critical for transcription-dependent plasticity. Signal order is crucial, and efficiency peaks when Ca²+ precedes V Δ C by 10–20 seconds—reminiscent of Hebbian plasticity algorithms, but \sim 1,000-fold prolonged. In Ca $_{\rm V}$ 1.2 Timothy syndrome mutants, the approach suggests that V Δ C mistuning is necessary for autistic symptoms, whereas Ca²+ overload suffices for cardiac phenotype.

M.R. Tadross and B. Li contributed equally to this work. Correspondence to Richard W. Tsien: richard.tsien@nyumc.org

31. A Plasma Membrane AKAP79/PKA/STIM1/Orai Complex Enables Phosphorylation of a Single Threonine in STIM1 to Provide a "Physiological Switch" for Calcium Release–independent Orai Channel Activity. JILL THOMPSON and TREVOR SHUTTLEWORTH, Department of Pharmacology and Physiology, University of Rochester Medical Center, Rochester, NY 14642

Endogenous mammalian Orai proteins form two distinct channels: store-operated CRAC channels formed by Orai1, and store-independent heteromeric Orai1/Orai3 ARC channels. Both channels require STIM1 for their activation but, whereas ER-located STIM1 activates CRAC channels, ARC channels are regulated by the minor pool of STIM1 resident in the PM. Importantly, STIM1 was originally identified as a PM-located phosphoprotein, and we have shown that ARC channel activity is PKA dependent (Mignen et al. 2013. *J. Physiol.* 567:787–798). Given these earlier findings, we investigated potential PKA-dependent phosphorylation sites within STIM1 and their possible role(s), along with the involvement of AKAP79 in this activity.

In silico analysis of the STIM1 cytosolic domain (residues 234-685) revealed several potential PKA-dependent sites. However, deletion of residues beyond H448 eliminates most of these without affecting STIM1's ability to activate endogenous ARC and CRAC channels, leading us to focus on a strongly indicated PKA site at residue T389. In vitro hyperphosphorylation analysis of an expressed STIM1-Δ448 construct revealed T389 as a genuine PKA site. Mutating T389 to a glutamate (mimicking phosphorylation) enabled normal ARC channel activity but essentially eliminated CRAC channel activity. Mutation to an alanine (mimicking the dephosphorylated state) allowed normal CRAC channel activity while eliminating ARC channel activity. Immunofluorescence and FRET studies showed that these effects were not caused by any obvious redistribution of STIM1 between ER and PM locations, and "forcing" the T389A mutant to the PM (via an N-terminal Lck sequence attached to the STIM1 cytosolic domain) failed to restore ARC channel activation. Furthermore, expression of an AKAP79 lacking the PKA-binding region markedly reduced ARC channel currents but was without effect on such currents in cells expressing the T398E mutant STIM1. Finally, FRET studies revealed significant interactions between AKAP79 and both STIM1 and Orai3, indicating a constitutive multi-molecular assembly of STIM1, AKAP79, and the ARC channel at the PM.

Note: The above findings have recently appeared in Thompson and Shuttleworth (2015. *J. Physiol.* 593: 559–572).

32. Conformational Dynamics of a Class C G Protein-coupled Receptor. REZA VAFABAKHSH,¹ JOSHUA LEVITZ,¹ and EHUD Y. ISACOFF,^{1,2,3} ¹Department of Molecular and Cell Biology and ²Helen Wills Neuroscience Institute, University of California, Berkeley, Berkeley, CA 94720; ³Physical Bioscience Division, Lawrence Berkeley National Laboratory, Berkeley, CA 94720

Metabotropic glutamate receptors (mGluRs) are dimeric class C G protein-coupled receptors and are expressed broadly, yet specifically, throughout various membrane compartments of neurons and glial cells. MGluRs are involved in the regulation of transmitter release in glutamatergic synapses as well as GABAergic and dopaminergic systems; modulate neuronal excitability, synaptic transmission, and plasticity; and serve as drug targets for neurological disorders. We used single-molecule fluorescence resonance energy transfer (smFRET) to probe the activation mechanism of fulllength mammalian mGluRs (mGluR2 and mGluR3). We find that the ligand-binding domains interconvert between three conformational states: resting, activated, and a short-lived intermediate state. Different orthosteric agonists induce transitions between the same conformational states with efficacy determined by the degree of occupancy of the active state. In the absence of glutamate, mGluR2 is inactive; however, mGluR3 displays basal dynamics, which are Ca2+ dependent and lead to spontaneous receptor activation. Our results support a general mechanism for the activation of mGluRs in which agonist binding induces closure of the ligand-binding domains followed by reorientation of the dimer interface. Our experimental strategy is easily adaptable to high resolution study of conformational dynamics in G protein-coupled receptors and other membrane proteins.

33. The Role of TMEM16E/Anoctamin 5 in Muscular Dystrophy and Phospholipid Scrambling. JARRED M. WHITLOCK, KUAI YU, YUAN YUAN CUI, DANIELLE GRIFFIN, LOUISE RODINO-KLAPAC, and H. CRISS HARTZELL, Department of Cell Biology, Emory University, Atlanta, GA 30322; Nationwide Children's Hospital, Ohio State University, Columbus, OH 43210

Deficits in muscle mass and strength associated with human muscular dystrophies have serious impacts on quality of life and longevity. Recently, recessive mutations in TMEM16E (Anoctamin 5) have been directly linked to a variety of different muscle diseases including limb-girdle muscular dystrophy type 2L (LGMD2L) and Miyoshi muscular dystrophy type 3 (MMD3); however, the underlying pathogenic mechanisms have remained elusive. TMEM16E is a member of the TMEM16/ Anoctamin superfamily that encodes both ion channels and regulators of membrane phospholipid scrambling. The phenotypic overlap of TMEM16E/ANO6 myopathies with dysferlinopathies (LGMD2B and MMD1) has inspired the hypothesis that TMEM16E may be involved in muscle membrane repair and progenitor cell fusion required to repair/regenerate muscle fibers damaged during injury. Here, we characterize a TMEM16E knockout mouse and show that TMEM16E-deficient mice demonstrate muscle phenotypes reminiscent of LGMD2L. The TMEM16E knockout mice exhibit significant exercise intolerance highlighted by their inability to run at a consistent pace. Additionally, muscle fibers from TMEM16E knockouts contain numerous inclusions that are not observed in wild-type tissue, which is also characteristic of LGMD2L. Muscle fibers exhibit a reduced capacity to repair the sarcolemma after laser damage and display defective muscle regeneration after injury. Moreover, we characterize a myoblast fusion defect impeding cell-cell fusion to produce multinucleated muscle fibers. We hypothesize that these defects are caused by defective phospholipid scrambling mediated by ANO5. This scramblase activity exposes phosphatidylserine on the outer leaflet of the membrane, a step that is required at sites of myoblast fusion to produce multinucleated myofibers. In support of this hypothesis, we find that TMEM16E expression elicits Ca²⁺-dependent phospholipid scrambling. We propose that TMEM16A/ANO5 myopathy is caused by defective phospholipid scrambling normally elicited by TMEM16E at the plasma membrane during myogenic regeneration/repair.

34. Cardiomyocyte-specific Leucine-rich Repeat-containing 10 (Lrrc10) Protein Regulates Ca_v1.2 l-type Ca²⁺ Channel Function in the Heart. MARITES T. WOON,¹ PAMELA LONG,³ LOUISE REILLY,¹ LI FENG,¹ COURTNEY R. REYNOLDS,¹ YOUNGSOOK LEE,² TIMOTHY OLSON,³ and RAVI C. BALIJE-PALLI,¹¹Cellular & Molecular Arrhythmia Research Program, Department of Medicine, and ²Department of Cell and Regenerative Biology, University of Wisconsin, Madison, WI 53706; ³Cardiovascular Genetics Research Laboratory, Mayo Clinic, Rochester, MN 55905

L-type Ca²⁺ channels (LTCCs) regulate multiple cellular processes including excitation–contraction coupling, signaling, and gene expression in the heart. Dysregulation of LTCCs is implicated in many cardiovascular diseases, including atrial fibrillation, dilated cardiomyopathy (DCM), and heart failure. Leucinerich repeat-containing 10 (LRRC10) was identified as cardiac-specific protein, which plays critical roles in

heart development and function. Recently, we have shown that hearts from Lrrc10-null $(Lrrc10^{-/-})$ mice develop DCM and exhibited reduced LTCC current (I_{Ca.L}). Subsequently, a homozygous mutation in the LRRC10 gene (I195T) was identified in a pediatric DCM patient. It is unclear how LRRC10 or the DCM-linked LRRC10 mutation impacts LTCC function. We investigated the role of LRRC10 and the DCM-linked mutation I195T in the regulation of LTCCs by coexpressing the wild-type (WT) LRRC10 or the LRRC10I195T with LTCC comprised of Ca_v1.2, β_{2CN2} , and $\alpha_2\delta$ subunits in HEK293 cells, and performed whole-cell patch-clamp experiments. Coexpression of LRRC10WT significantly enhanced the peak $I_{Ca,L}$ density (-81 ± 5 pA/pF) and shifted the voltage dependence of activation of I_{Ca,L} to hyperpolarized potentials ($V_{1/2}$ of -16.6 ± 1.3) compared to control LTCC ($-34 \pm 2 \text{ pA/pF}$; $V_{1/2}$ of -13.6 ± 0.9). In contrast, coexpression of LRRC10I195T significantly reduced the $I_{Ca,L}$ (-18 \pm 3 pA/pF) and activation to depolarized potentials ($V_{1/2 \text{ of}} - 8.9 \pm 0.5$). Coexpression of LRRC10I195T significantly shifted the steady-state inactivation of $I_{Ca,L}$ to depolarized potentials ($V_{1/2}$ of $-24.4 \pm$ 1.8) and enhanced the window current compared to LRRC10WT ($V_{1/2}$ of -29.2 ± 1.6). Coimmunoprecipitation analyses in the mouse hearts and transiently expressed HEK293 cells revealed that both WT and LRRC10I195T specifically associate with Ca_v1.2 subunit, but not the $Ca_{\nu}\beta_{9}$ subunit. We conclude that LRRC10 interacts with the Ca_v1.2 subunit and regulates LTCC function by enhancing the density and biophysical properties of $I_{\text{Ca,L}}$. The DCM-linked LRRC10I195T mutation reduces the I_{Ca,L} and enhances the window current, which may contribute to arrhythmia and cardiac dysfunction in DCM patients.

Sponsor: Ravi C. Balijepalli

35. Structure and Selectivity in Bestrophin Ion Channels. TINGTING YANG,¹ QUN LIU,³ BRIAN KLOSS,⁴ RENATO BRUNI,⁴ RAVI C. KALATHUR,⁴ YOUZHONG GUO,¹ EDDA KLOPPMANN,⁴,⁵ BURKHARD ROST,⁴,⁵ HENRY M. COLECRAFT,² and WAYNE A. HENDRICKSON,¹,²,3,⁴ ¹Department of Biochemistry and Molecular Biophysics and ²Department of Physiology and Cellular Biophysics, Columbia University, New York, NY 10032; ³New York Structural Biology Center, Synchrotron Beamlines, Brookhaven National Laboratory, Upton, NY 11973; ⁴NYCOMPS, New York Structural Biology Center, New York, NY 10027; ⁵Department of Informatics, Bioinformatics and Computational Biology, TUM (Technische Universität München), Garching 85748, Germany

Human bestrophin 1 (hBest1) is a calcium-activated chloride channel from the retinal pigment epithelium, where mutations are associated with vitelliform macular degeneration, or Best disease. We describe the structure of a bacterial homolog (KpBest) of hBest1 and functional

characterizations of both channels. KpBest is a pentamer that forms a five-helix transmembrane pore, closed by three rings of conserved hydrophobic residues, and has a cytoplasmic cavern with a restricted exit. From electrophysiological analysis of structure-inspired mutations in KpBest and hBest1, we find a sensitive control of ion selectivity in the bestrophins, including reversal of anion/cation selectivity, and dramatic activation by mutations at the cytoplasmic exit. A homology model of hBest1 shows the locations of disease-causing mutations and suggests possible roles in regulation.

36. Human Stem Cell Model of Cardiac Calcium Channelopathy. MASAYUKI YAZAWA, *Rehabilitation* and Regenerative Medicine, Pharmacology, Columbia University, New York, NY 10032

A human-induced pluripotent stem cell-based model of inherited diseases has been proved to be useful for identifying new therapeutics. However, the use of a human stem cell-based model of cardiac diseases is still hampered by the high cost and complexity of methods used for reprogramming, in vitro differentiation, and phenotyping, and also by immature features of generated cells such as cardiomyocytes. To address these limitations, we first optimized a protocol for reprogramming of human fibroblasts and keratinocytes into pluripotency using single lipofection and the episomal vectors in 24/96-well plate format. This method allowed us to generate multiple lines of integration-free and feederfree induced pluripotent stem cells from multiple patients and controls. Second, using our new monolayer differentiation method, we generated human cardiomyocytes from Timothy syndrome patients who have a missense mutation in CACNA1C gene encoding L-type voltage-gated calcium channel Ca_v1.2, causing severe cardiac arrhythmia. We found that Timothy syndrome cardiomyocytes showed slower, irregular contractions and abnormal calcium handling compared with controls. Third, we developed efficient approaches for recording action potentials, calcium currents, and calcium transients in control and patient cardiomyocytes using genetically encoded fluorescent indicators and automated patch-clamp devices. We confirmed that roscovitine rescued the phenotypes in action potentials, channel inactivation, and calcium handling in Timothy syndrome cardiomyocytes. These findings were consistent with previous studies using conventional electrophysiological recordings and calcium imaging with dyes (Yazawa et al. 2011. Nature. 471:230-234). Fourth, using these approaches, we have investigated novel molecules involved in the pathogenesis of Timothy syndrome. In addition, we tested 20 roscovitine analogs and found that three out of the candidates could rescue the phenotypes in Timothy syndrome cardiomyocytes. The approaches using our optimized methods and recordings will improve applicability of human stem cell models for disease study to test potential therapeutics.

37. Identification of a Lipid Scrambling Domain in ANO6/TMEM16F. K. YU, J.M. WHITLOCK, Y. YUAN CUI, and H.C. HARTZELL, *Department of Cell Biology, Emory University School of Medicine, Atlanta, GA 30322*

Phospholipid species in the membranes of eukaryotic cells are asymmetrically distributed between the two leaflets. The collapse of this asymmetry, termed "phospholipid scrambling" (PLS), is a ubiquitous signaling mechanism involved in various processes including recognition of apoptotic cells by phagocytes, blood clotting, and formation of multinucleated cells like striated myofibers. Recently, it was discovered that ANO6/ TMEM16F is required for Ca²⁺-dependent PLS. However, there is considerable controversy over whether ANO6 is itself a phospholipid scramblase (PLSase) and/or an ion channel like other members of the ANO family. Here, we have combined patch-clamp recording with simultaneous measurement of PLS to study the role of ANO6 in phospholipid scrambling. We show that ANO6 elicits robust Ca2+-dependent PLS that coincides with ionic currents. We believe these currents are explained by ionic leak that occurs during phospholipid translocation because they are nonselective and coincide temporally with the development of PLS. PLS is not dependent on these currents and occurs when there is no electrochemical driving force for any ion. Further, we have identified a domain in ANO6 (encompassing parts of transmembrane domains 4 and 5) that is essential for PLS and is sufficient to confer PLS activity on ANO1, which normally does not scramble. Homology modeling of ANO6 based on the recently solved structure of the fungal TMEM16, nHTMEM16, shows that the scramblase domain lines an unusual hydrophilic cleft that faces the lipid bilayer. Mutagenesis of ANO1 suggests that this cleft is also involved in Cl permeation, raising the idea that the Cl pore of ANO1 and the PLS pathway of ANO6 have structural similarity. ANO5, a paralog with 75% similarity to ANO6, also exhibits robust PLS activity, although certain features differ from ANOP6-mediated PLS. These observations provide insights into the ion channel and phospholipid scrambling functions of the anoctamin/TMEM16 family.

38. Coupling of Distinct Ion Channel Types in Neurons Mediated by AKAP79/150. JIE ZHANG and MARK S. SHAPIRO, *University of Texas Health Science Center at San Antonio, San Antonio, TX 78229*

M-type K⁺ channels, comprised of KCNQ2-5 subunits, play key roles in the regulation of neuronal excitability in the peripheral and central nervous systems. In diverse neurons, L-type Ca²⁺ channels (LTCCs) drive transcriptional regulation via NFAT transcription factors, and in sensory neurons, TRPV1 cation channels excite

neurons in response to heat, acidity, or chemical ligands, driving nociception. The A kinase-anchoring protein (AKAP)79/150 has been shown to orchestrate regulation of all three types of channels by PKC, PKA, calcineurin, or NFAT transcription factors. Using stochastic optical reconstruction microscopy (STORM), which offers sub-diffraction (\sim 20-nm) resolution, we have directly visualized individual signaling complexes containing endogenous and cloned AKAP79/150, these three ion channels, and G protein-coupled receptors in neurons and tissue culture cells. We also observed AKAP150-mediated clustering of KCNQ, LTCCs, and TRPV1 channels at the single-complex level. Thus, AKAP79/150 links different channel types together, raising the possibility of their functional, as well as physical, coupling. In neurons isolated from AKAP150+/+ mice, brief application of low concentrations of capsaicin (100 nM), which we believe to trigger local PIP₂ depletion, induced ~40% suppression of M-current amplitude (I_M) , suggesting close localization of TRPV1 and M channels. However, in AKAP150-/- neurons, I_M was not affected by such modest activation of TRPV1 channels, implying the critical role of AKAP79/150 in bringing together these two ion channels. Preincubation of cells with thapsigargin to deplete stores had no effect. Furthermore, with the application of the LTCC blocker, nifedipine, but not the N-type Ca2+ channel blocker, ω -conotoxin GVIA, I_M was significantly suppressed, and both acute desensitization and tachyphylaxis of TRPV1 currents were greatly impaired, suggesting the functional coupling of LTCCs with KCNQ, and TRPV1 channels, consistent with our findings suggesting their physical coupling at the single-complex level with STORM.

39. Internally Translated GJA1-20k Contributes Specificity to Gap Junction Delivery. SHAN-SHAN ZHANG, TINGTING HONG, and ROBIN SHAW, Cedars-Sinai Medical Center and University of California, Los Angeles, Los Angeles, CA 90095

Introduction

Delivery of connexin 43 (Cx43) to the cardiac intercalated disc is a continuous and rapid process critical for intercellular coupling. We have found that EB1-tipped microtubules can deliver Cx43 hemichannels directly to adherens junctions (Shaw et al. 2007. *Cell.* 128:547–560; Smyth et al. 2010. *J. Clin. Invest.* 120:266–279). More recently, we have identified that actin assists with forward trafficking (Smyth et al. 2012. *Circ. Res.* 110:978–989), and that Cx43 hemichannels have newly recognized accessory subunits that are truncated isoforms derived from internal translation. The 20-kD isoform (GJA1-20k) is required for full-length Cx43 localization to the plasma membrane (Smyth and Shaw. 2013. *Cell. Rep.* 5:611–618). In this study, we asked how GJA1-20k contributes specificity to Cx43-targeted delivery.

Hypothesis

GJA1-20k organizes cytoplasmic actin cytoskeleton to orient microtubules and localize full-length Cx43 delivery.

Methods and Results

Using HeLa and neonatal ventricular myocyte expression systems, we find that GJA1-20k is distributed among dynamic reticular and punctate structures. Immunolabeling with anti-protein disulfide isomerase and live-cell imaging with reticulon 4 (rtn4a-GFP) confirm the presence of GJA1-20k in the endoplasmic reticulum. GJA1-20k—positive reticular structures form contact points with the actin cytoskeleton, through which microtubules appear and traverse. We find that GJA1-20k not only interacts with F-actin but also stabilizes F-actin polymerized in vitro. Disruption of F-actin with latrunculin A results in impaired EB1-based microtubule attachment to micropatterned cell–cell junctions, as well as decreased Cx43 localization. Exogenous GJA1-20k rescues latrunculin A—induced altered trafficking.

Conclusions

Collectively, these results indicate that the internally translated GJA1-20k isoform interacts with F-actin to organize growth trajectories of the microtubule delivery machinery, directing full-length protein traffic toward the cellular junction.

40. Molecular Pathology of Sodium Channel B1 Subunit Mutations That Are Linked to Atrial Fibrillation. WANDI ZHU, BICONG LI, and JONATHAN R. SILVA, *Washington University in St. Louis, St. Louis, MO 63130*

Background

In cardiomyocytes, $Na_v1.5$ coassembles with β subunits, which modulate channel gating, surface expression, and posttranslational modification. β -subunit mutations can cause Brugada syndrome, long-QT syndrome, and atrial fibrillation (AF). We aim to assess molecular mechanisms of β 1-subunit regulation of $Na_v1.5$ and its pathological modification by AF variants.

Methods

The $\mathrm{Na_V}1.5~\alpha$ subunit contains four domains (DI–DIV), each with a voltage-sensing domain (VSD). We previously created four DNA constructs that each contain a cysteine within a single VSD. Channels encoded by these constructs were expressed in *Xenopus laevis* oocytes, and cysteines were labeled with TAMRA-MTS fluorophores. Ionic current and VSD-tracking fluorescence emission were simultaneously recorded using the cut-open configuration.

Results

Compared to α alone, coexpression of WT-β1 causes a hyperpolarizing steady-state inactivation shift without affecting activation. WT-β1 does not affect the DI-DIII VSDs, while significantly depolarizing the DIV fluorescence-voltage (FV) relationship, which correlates with the inactivation shift (+ β_1 : FV – V_{1/2} = -52.4 \pm 2.0; – β_1 : $FV - V_{1/2} = -89.5 \pm 3.3 \text{ SEM}$; P = 0.007). Compared to WT-β1, AF mutant β1-R85H induces a depolarizing activation shift, modest hyperpolarization of inactivation, and hyperpolarization of both the DIII- and DIV-FVs (DIII-FV: +WT- β_1 V_{1/2} = -106.1 ± 3.2; +R85H- β 1: V_{1/2} = -118.6 ± 2.9 ; P = 0.034; DIV-FV: +R85H- β_1 V_{1/2} = $-60.7 \pm$ 0.5; P = 0.03). Thus, the R85H mutant induces β_1 DIII-VSD modulation that is not observed with WT-β1. The D153N-β1 AF variant also displayed a unique phenotype, hyperpolarizing activation, depolarizing inactivation, and hyperpolarizing DIV-VSD activation versus WT-β1 $(+D153N-\beta_1: V_{1/2} = -63.96 \pm 0.2; P = 0.01).$

Conclusions

Our results imply that the WT- β_1 subunit nominally regulates channel inactivation by modulating DIV-VSD activation. R85H causes opposite shifts in channel activation and DIII/DIV-VSD activation, suggesting a decoupling of channel pore and the DIII/DIV-VSD. D153N induces a hyperpolarizing shift in DIV-VSD activation, but a depolarizing shift in channel inactivation, indicating disruption of DIV-VSD inactivation regulation. Collectively, our results show that $\beta1$ AF mutations have unique molecular pathologies that are likely to impact patient phenotypes and therapeutic response.

INDEX OF AUTHORS

Agullo-Pascual, E., 1, 17 Anumonwo, J., 27 Archer, C.R, 2 Arcos, T., 1 Balijepalli, R.C., 34 Barca, E., 13 Ben-Johny, M., 3 Bin, L., 1 Bonev, A.D., 8, 12 Brayden, J.E., 4 Bruni, R., 35 Bu, L., 1 Calebiro, D., 21 Calkins, H., 1 Campbell, S.G., 15 Catalán, M.A., 25 Caudillo-Cisneros, C., 22 Cerrone, M., 1 Chang, D.D., 29 Colecraft, H.M., 13, 14, 20, 29, 35 Collier, D.M., 8 Cui, Y.Y., 33, 37 Dabertrand, F., 4, 18 Del Pilar Gomez, M., 11, 16 Delmar, M., 1, 17 Dick, I.E., 5 Duran, S., 16 Ehrlich, B.E., 15 Enslow, B.T., 2 Feng, L., 34 Fenyo, D., 17 Ferguson, D., 28 Forrester, F.M., 6 Fowler, S., 1 Franck, J., 7 Freeman, K., 8, 12 Fu, D., 23 Fu, Y., 9 Galindo, C., 11 Gargus, J.J., 28 Gomez, L., 23 Gonzales, A.L., 10, 18 González, K., 11 Good, S., 7 Gorelik, J., 17 Griffin, D., 33 Guerrero-Serna, G., 27 Guo, Y., 35 Harraz, O.F., 12 Hartzell, H.C., 33, 37 Hendrickson, W.A., 35 Herron, T., 27

Hurst, S., 23 Ibrahim, M., 27 Isacoff, E.Y., 32 James, C.A., 1 Jaramillo, Y., 25 Jhun, B.S., 23 Joseph, L.C., 13, 14 Joshi-Mukherjee, R., 5 Judge, D.P., 1 Kalathur, R.C., 35 Kats, I., 19 Keegan, S., 17 Kittel, R.J., 21 Kloppmann, E., 35 Kloss, B., 35 Koide, M., 18 Komrowski, M., 13 Korchev, Y.E., 17 Kotlikoff, M.I., 10 Kumar, K., 28 Kuo, I.Y., 15 Kwaczala, A.T., 15 Lacampagne, A., 6 Landinez, M.P., 16 Lee, Y., 34 Leo-Macias, A., 17 Levitz, J., 32 Li, B., 30, 40 Liang, F.-X., 17 Lin, X., 1, 17 Liu, Q., 35 Lohse, M.J. 21 Long, P., 34 Longden, T.A., 10, 12, 18 Ma, H., 19 Ma, S., 20 Maiellaro, I., 21 Marks, A.R., 6 Márquez-Gamiño, S., 22 Melvin, J.E., 25 Mishra, J., 23 Morrow, J.P., 13, 14 Murray, B., 1 Musa, H., 27 Naami, R., 9 Nasi, E., 11, 16 Ndukwe, T., 27 Nelson, M.T., 4, 8, 10, 12, 18 Nguyen, L., 15 Nguyen, R.L., 28 Obregón-Herrera, A., 22 Olcese, R., 24

Olson, T., 34

Onetti, C.G., 22

Osorno, T., 16 O-Uchi, J., 23 Pantazis, A., 24 Parker, I., 28 Pellisier, T., 7 Peña-Münzenmayer, G., 25 Pennefather, P., 26 Reed, P.A., 2 Reiken, S., 6 Reilly, L., 34 Reynolds, C.R., 34 Rodino-Klapac, L., 33 Rosinski, B., 27 Rost, B., 35 Rothenberg, E., 1, 17 Sackheim, A., 8 Sanchez, S., 19 Sanchez-Alonso, J.L., 17 Schmunk, G., 28 Shapiro, M.S., 2, 38 Shaw, R., 39 Shaw, S., 9 Sheu, S.-S., 23 Shui, B., 10 Shuttleworth, T., 31 Silva, J.R., 40 Sonkusare, S.K., 12 Subramanyam, P., 13, 14, 29 Suhanic, W., 26 Suutari, B., 19 Tadross, M.R., 30 te Riele, A.S., 1 Thompson, J., 31 Tichnell, C., 1 Tsien, R.W., 19, 30 Umanskaya, A., 6 Vafabakhsh, R., 32 Vera-Delgado, K.S., 22 Villalba, N., 8 Vuong, C., 9 Whitlock, J.M., 33, 37 Woon, M.T., 34 Xie, W., 6 Yang, T., 35 Yang, W., 5 Yazawa, M., 36 Yegorov, S., 7 Yu, K., 33, 37 Yue, D.N., 3 Yue, D.T., 3, 5 Zhang, J., 38 Zhang, M., 1 Zhang, S.-S., 39 Zhu, W., 40

Hirano, M., 13

Hong, T., 9, 39